

Influence of the B-site cation nature on crystal structure and magnetic properties of Ca_2BMoO_6 (B = Cr, La, Sm) double perovskite

Ioana A. Gorodea^{a*}

^a *Department of Chemistry, "Al. I. Cuza" University of Iasi,
11 Carol I Bd, Iasi 700506, Romania*

Abstract: Double perovskite-type oxide Ca_2BMoO_6 materials, where B = Cr, La and Sm, were prepared by the sol-gel auto-combustion method for the first time. The role of different B-site cations on their synthesis, structures, and magnetic properties was investigated. The synthesis progress was followed by the Fourier transform infrared spectroscopy and the samples' structure was investigated by X-ray diffraction. The increase of the ionic radii B leads to the decrease of the t-value which reflects the structural distortion from the ideal cubic perovskite. Magnetization measurements were made with a SQUID magnetometer. All compounds are ferimagnetic and magnetic properties are indirectly influenced by the distortion degree of the lattice and disorder on the B/B' positions.

Keywords: Double-perovskite; Sol-gel auto-combustion; X-ray diffraction; FT-IR spectroscopy; Magnetic properties

Introduction

Complex metal oxides with the general formula $\text{A}_2\text{B}'\text{B}''\text{O}_6$, where B' and B'' sites are occupied alternately by different cations, depending on

* Ioana A. Gorodea, *e-mail:* gorodea@uaic.ro

their valences and relative ionic radii, are known as double perovskites or epsolites.¹ The perovskite type oxides have some flexibility in the chemical composition and crystal structure; the combination of many kinds of ions and the control of their crystal structure are possible. The modification of structural and magnetic properties by changing the A, B' and/or B'' site cations has gained interest in recent years in order to better understand the mechanism of colossal magnetoresistance.² If in the unit cell of a perovskite structure exist two cations ordered on the B site this is becoming a unit cell of a double perovskite structure as in $AB_{0.5x}B'_{0.5-0.5x}O_3$, which corresponds to the well known formula $A_2B'_xB''_{1-x}O_6$.

Also the double-perovskite compounds which containing magnetic ions in positions B were synthesized and they proved to have important technological applications.^{3,4} In general, the size of A ion influences the crystal symmetry significantly while that of the B ion does not change the symmetry, but changes the lattice volume proportionally.^{5,6}

In order to improve the properties of double perovskites and to obtain the appropriate products for different applications, various synthesis techniques such as sol–gel,⁷ hydrothermal,⁸ or co-precipitation⁹ have been developed. Among these methodologies, sol–gel and its variants, including sol–gel autocombustion, has been shown to have great potential in the preparation of metal oxides with the perovskite structure for advanced applications.¹⁰

The aim of this work was to obtain a series of double perovskite oxides Ca_2BMoO_6 (B = Cr, La, Sm) for the first time. Also, a study on the effect of these three trivalent B-site cations on the phase formation by the sol–gel autocombustion method, structural characteristics, and magnetic properties is presented.

Experimental

Samples of Ca_2BMoO_6 were prepared using the sol–gel autocombustion method by mixing $\text{Ca}(\text{NO}_3)_2 \cdot 4\text{H}_2\text{O}$, $\text{Cr}(\text{NO}_3)_3 \cdot 9\text{H}_2\text{O}$, $\text{La}(\text{NO}_3)_3$, $\text{Sm}(\text{NO}_3)_3 \cdot 6\text{H}_2\text{O}$, $(\text{NH}_4)_6\text{Mo}_7\text{O}_{24} \cdot 4\text{H}_2\text{O}$ with citric acid as the combustion agent. The metallic precursors and citric acid were dissolved in distilled water and the mixtures were gradually heated up to 80°C / 4 h under continuous stirring in a water bath in order to obtain a viscous gel. After slow evaporation at $80 - 90^\circ\text{C}$, the obtained gel was dried in air up to 220°C , until the autocombustion took place.

The thermal treatment was carried out in air at $500^\circ\text{C}/7\text{h}$. The samples were pressed at 150 kPa into pellets of 10mm diameter and 2 mm thickness and sintered in air at $900^\circ\text{C}/7\text{h}$, $1100^\circ\text{C}/24\text{h}$ and $1200^\circ\text{C}/24\text{h}$.

This procedure (grinding, pelletizing and firing) was repeated until single-phase perovskite could be obtained. The disappearance of nitrate and carbonate phases and the phase formation of the double perovskite Ca_2BMoO_6 (B = Cr, La, and Sm) was monitored by using a Fourier transform infrared (FTIR) spectra analysis of crystalline structure and identification of perovskites phases was performed by means of X-ray diffraction technique.

X-ray diffraction (XRD) patterns of the sample were recorded with a SHIMADZU LabX6000 diffractometer equipped with a graphite monochromator and $\text{CuK}\alpha$ radiation ($\lambda = 1.5406 \text{ \AA}$). The samples mounted in reflection mode were analyzed in ambient atmosphere with scanning rate of $0.02^\circ \text{ s}^{-1}$ over the $2\theta = 20\text{--}80^\circ$ range.

IR spectra were obtained using a JASCO 660 PLUS spectrophotometer with wave number range $4000 - 400 \text{ cm}^{-1}$ and used to complete the structure studies. The samples were mixed with KBr in the

mass ratio 0.04:1, and then compacted into pellets with a thickness of 0.5 - 0.75 mm and a diameter of 13 mm under a pressure of 0.3 GPa in atmospheric air.

Magnetization data were collected with a Quantum Design MPMS-XL superconducting quantum interference device (SQUID) magnetometer. Temperature-dependent magnetization data were recorded at various applied magnetic fields (H) in the temperature range $2 < T$ (K) < 400 after cooling the sample in zero magnetic field (zero-field-cooled, ZFC) and while cooling in the presence of the field (field-cooled, FC). Field and zero field cooled magnetizations were measured on a Quantum Design SQUID magnetometer. The sample sizes were 100-200 μ g and were packed into teflon tape packet.

Results and discussion

The X-ray powder diffraction profiles collected for Ca_2BMoO_6 (B = Cr, La, Sm) are shown in figure 1. The recorded patterns present sharp and well-defined peaks, indicating that the as prepared materials have a highly crystalline nature.

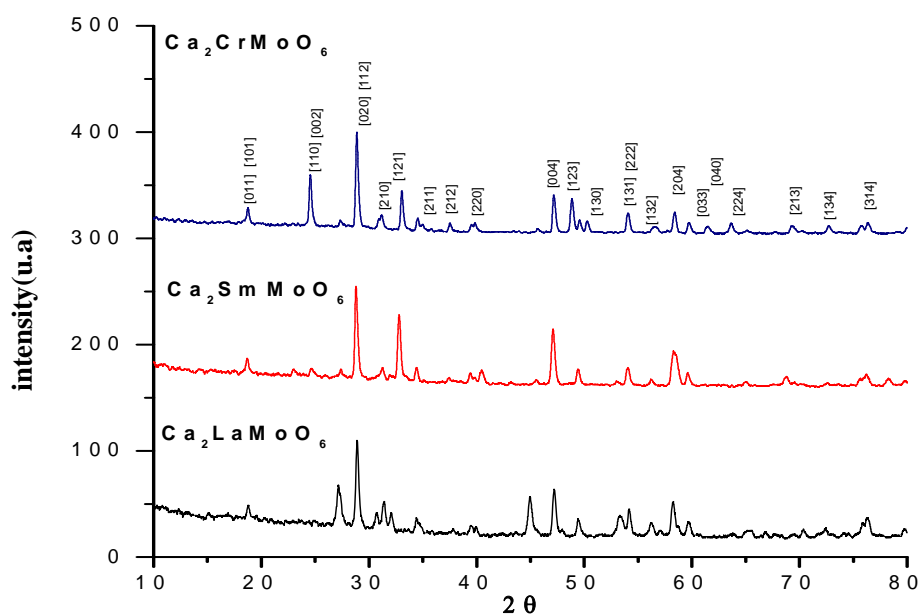


Figure 1. X-ray diffraction patterns of Ca_2BMoO_6 .

The strongest reflection peaks at 2θ of around 30° , assigned to the (112), (110) and (220) diffraction planes, were identified in the pattern of each sample, confirming the formation of the double perovskites phase.¹¹ In the case of Ca_2BMoO_6 where $\text{B} = \text{Cr}$, all the peaks in the XRD pattern fit well to a orthorhombic unit cell with $Pbnm$ space group. Samples of Ca_2BMoO_6 where $\text{B} = \text{Sm}$ and La have a monoclinic structure with the space group $P/2_1/n$.

Structural parameters: tolerance factor (t), lattice parameters, cell volume (V), cell angle (β) evaluated using Structure Prediction Diagnostic Software (SPuDs)¹² are summarized in Table 1.

Table 1. Crystallographic data calculated from SPuDS for powders sintered at 1200°C .

Compound	$r_{B^{3+}}$ (Å)	t space group	Cell parameter (Å)	$V(\text{Å}^3)$	$\beta(^{\circ})$
$\text{Ca}_2\text{CrMoO}_6$	0.52	0.9404 $Pbnm$	$a = 5.3913 \text{ \AA}$, $b = 5.5266 \text{ \AA}$, $c = 7.7161 \text{ \AA}$	229.906	89.999 5
$\text{Ca}_2\text{SmMoO}_6$	0.964	0.8612 $P21/n$	$a = 5.5178 \text{ \AA}$, $b = 5.9179 \text{ \AA}$, $c = 8.0531 \text{ \AA}$	262.964	89.871 4
$\text{Ca}_2\text{LaMoO}_6$	1.061	0.8447 $P21/n$	$a = 5.5296 \text{ \AA}$, $b = 6.0038 \text{ \AA}$, $c = 8.1090 \text{ \AA}$	269.204	90.197 0

From Table 1 a monotonic increase of lattice parameters and, consequently, increase in cell volume with increase of the B site cationic effective ionic radii ($r_{\text{Cr}^{3+}} < r_{\text{Sm}^{3+}} < r_{\text{La}^{3+}}$) is observed. The increase of the effective ionic radii of the B cation leads to an increase of the tolerance factor which determines the transition from the orthorhombic structure to

the distorted monoclinic perovskite structure. It must be mentioned that the tilt angle and the tolerance factor give contribution to the structural distortion from the ideal cubic perovskite.¹³ When the tolerance factor value is smaller than the unity, the compound presents a structure with a lower symmetry, different from the cubic one.¹⁴

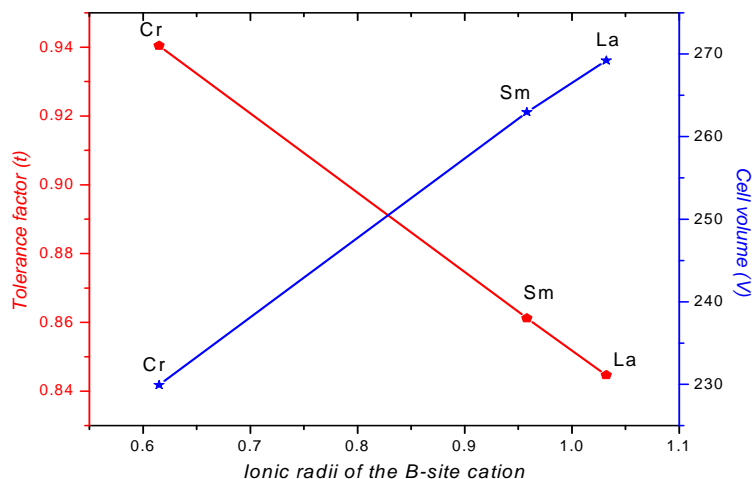


Figure 2. The variation of the tolerance factor (t) and cell volume (V) according to the ionic radii of the B site cation ($r_{B^{3+}}$).

In our case (figure 2) the tolerance factor increases with increasing of the ionic radius in the series ($r_{Cr^{3+}} < r_{Sm^{3+}} < r_{La^{3+}}$) and therefore can say that when $B = Cr$ we obtain perovskite-type orthorhombic structure with a high degree of order and symmetry

The FTIR spectra of the perovskite structure have three characteristics: absorption bands between $850 - 400 \text{ cm}^{-1}$, respective to composition which are usually used to identify the perovskite phase formation.¹⁵

The figure 3 clearly shows that all spectra present the typical band pattern characteristic of the perovskite structure between $850 - 400 \text{ cm}^{-1}$, one at high-wavenumber range (around 800 cm^{-1}), one at 600 cm^{-1} and one at lower range of wavenumber (around 430 cm^{-1}).

The strong high energy band centred at about 660 cm^{-1} can surely be assigned to the antisymmetric stretching mode of MoO_6 octahedra due to

higher charge of this cation, a band at 840 cm^{-1} which can be assigned to the symmetric stretching vibration of these octahedra and the strong IR-band at around 450 cm^{-1} which can be assigned to the Mo(B)O_6 deformation.

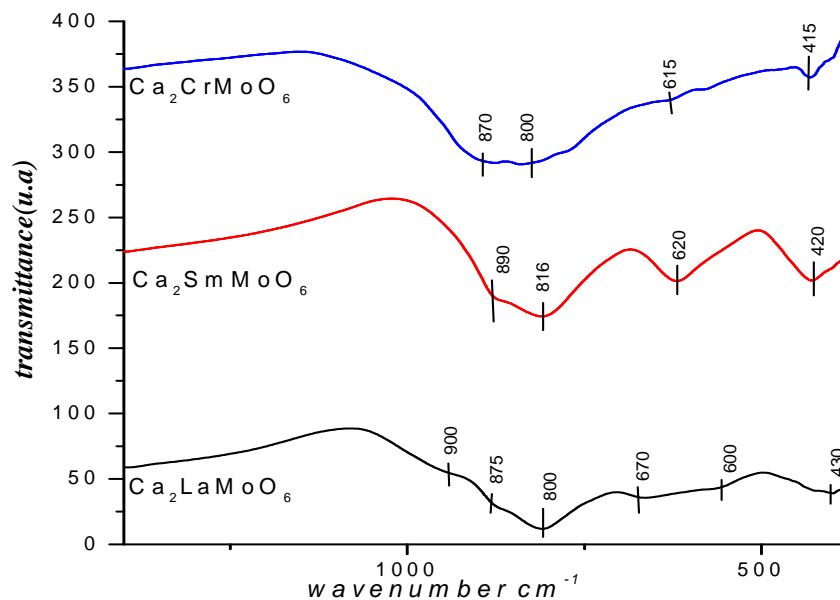


Figure 3. FT-IR spectra for the Ca_2BMoO_6 powders.

The size of the B cation seems to be relevant to the structural distortion; in our case the tolerance factor increases with the size of cation B and a low displacement of bands into at high wavenumber range was observed. For all the compounds with $\text{B} = \text{Cr}$, Sm and La , the presence of these bands confirm the formation of perovskite phase.

The plots of magnetization against temperature for Ca_2BMoO_6 ($\text{B} = \text{Cr}$, Sm) are also given in the upset of figure 4 a) and b). It is observed that for all compounds the magnetization decreases with increasing temperature and all compounds are ferrimagnetics.

It is also noted that the compound's $\text{Ca}_2\text{CrMoO}_6$ Curie temperature $T_c = 120\text{ K}$ is very similar to that reported in the literature for the compound $\text{Ca}(\text{Cr}_{0.5}\text{Mo}_{0.5})\text{O}_3$.¹⁶

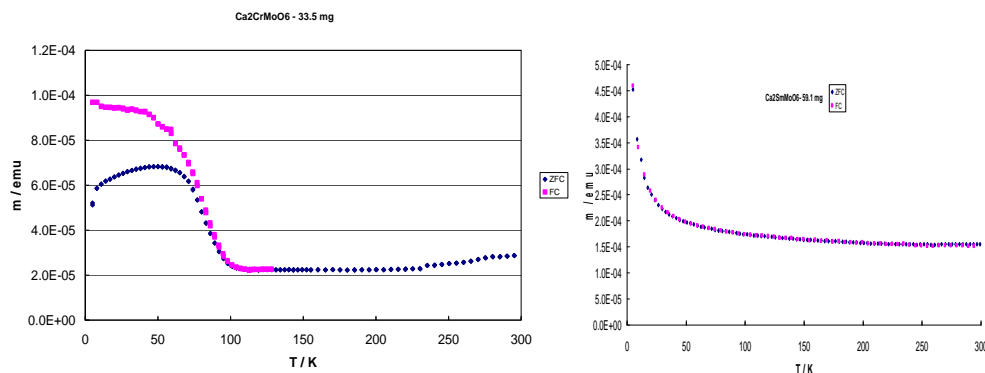


Figure 4. a) Variation of the specific magnetization with temperature of $\text{Ca}_2\text{CrMoO}_6$;
 b) Variation of the specific magnetization with temperature of $\text{Ca}_2\text{CrSmO}_6$.

As it can be seen, the magnetization of the samples decrease with increasing of the ionic radius B due to the site defects resulting from the partial disorder of B and Mo ions among the B'/B'' sublattices. The nature and origin of this decrease of the magnetization in the presence of disorder is still a matter of debate in the literature.

The disorder appears to be responsible for the low value of magnetization.

Conclusions

This study is the first to report on the synthesis of Ca_2BMoO_6 (B = Cr, Sm, La) double perovskites by the sol–gel autocombustion method with citric acid as the combustion agent. The synthesis method selected proved to be quite good, although in order to achieve the formation of perovskite phase without impurities is required a fairly high temperature sintering.

We have performed a detailed analysis of the influence of cation nature in the position B on the structural and magnetic characterization of the double perovskite. FTIR spectra and XRD patterns confirmed the double-perovskites phase formation for all obtained materials. Cell

parameters, volume, angle, and the bond length are influenced by the nature of the B-site cation as resulted from the SPuDS software.

From the point of view of the ideal perovskite, Cr cation proved to be the best position for cavity type B.

All compounds are ferrimagnetics and magnetic properties are indirectly influenced by the distortion degree of the lattice and disorder on the B/B' positions.

References

1. Andreson, M. T., Greenwood, K.B., Taylor, G.A., Poppelmeier, K. R. B-cation arrangements in double perovskite. *Progr. Solid State Chem.* **1993**, *22*, 197-233.
2. Kobayashi, K. I., Kimura, T., Sawada, H., Terakura, K., Tokura, Y. Room-temperature en magnetoresistance in an oxide material with an ordered double-perovskite structure. *Nature.* **1998**, *395*, 677-680.
3. Chan, T. S., Liu, R. S, Guo, G. Y., Hu, S. F., Lin, J. G., Lee, J.-F., Jang, L.-Y. Chang, C.-R., Huang, C. Y. Structural, electrical and magnetic characterization of the double perovskites Sr_2CrMO_6 (M = Mo, W): B' 4d-5d system. *Solid State Commun.* **2004**, *131*, 531-535.
4. Tian, S. Z., Zhao, J. C., Qiao, C. D., Ji, X. L., Jiang, B. Z. Structure and properties of the ordered double perovskites Sr_2MWO_6 (M=Co, Ni) by sol-gel route. *Mater. Lett.* **2006**, *60*, 2747-2750.
5. Choy, J.-H., Park, J.-H. Hong, S.-T., Kim, D.-K. Competition of covalency between $\text{Cr}^{\text{III}}\text{-O}$ and $\text{Ta}^{\text{V}}\text{-O}$ bonds in the perovskites $\text{Ca}_2\text{CrTaO}_6$ and $\text{Sr}_2\text{CrTaO}_6$. *J. Solid State Chem.* **1994**, *111*, 370-379.
6. Kanaiwa, Y., Wakeshima, M., Hinatsu, Y. Synthesis, crystal structure, and magnetic properties of ordered perovskites $\text{Sr}_2\text{LnTaO}_6$ (Ln = lanthanides). *Mater. Res. Bull.* **2002**, *37*, 1825-1836.
7. Brunckova, H., Medvecký, L., & Hvizdoš, P. Effect of substrate on phase formation and surface morphology of sol-gel lead-free KNbO_3 , NaNbO_3 , and $\text{K}_{0.5}\text{Na}_{0.5}\text{NbO}_3$ thin films. *Chem. Pap.* **2012**, *66*, 748-756.
8. Wu, L. Y., Ma, J. M., Huang, H. B., Tian, R. F., Zheng, W. J., & Hsia, Y. F. Hydrothermal synthesis and 121Sb Mossbauer characterization of perovskite-type oxides: $\text{Ba}_2\text{SbLnO}_6$ (Ln = Pr, Nd, Sm, Eu). *Mater. Charact.* **2010**, *61*, 548-553.
9. Jacobo, S. E. Novel method of synthesis for double perovskite $\text{Sr}_2\text{FeMoO}_6$. *J. Mater. Sci.* **2005**, *40*, 417-421.
10. Blosi, M., Albonetti, S., Dondi, M., Costa, A. L., Ardit, M., & Cruciani, G. Sol-gel combustion synthesis of chromium doped yttrium aluminum perovskites. *J. Sol-Gel Sci. Technol.* **2009**, *50*, 449-455.

11. Lavat, A. E. & Baran, J. E. Synthesis and characterization of $\text{Ca}_2\text{CoTaO}_6$, a new monoclinically distorted double perovskite. *Material Research*, **2011**, *14*, 472–472.
12. Lufaso, M. W & Woodward P.M. Prediction of the crystal structures of perovskites using the software program *SPuDS*. *Acta Crystallographica Section, B*. **2001**, *57*, 725-738.
13. Lin, Q., Greenblatt, M. Caspi, El'ad N. Avdeev, M. Crystallographic and magnetic properties of CaLaMnMoO_6 double perovskite, *J. Solid State Chem.* **2006**, *179*, 7 , 2086-2092.
14. Munoz, A., Alonso, J. A., Casais, M. T., Martinez-Lope, M. J., Fernandez-Diaz, M. T. Crystal and magnetic structure of the complex oxides $\text{Sr}_2\text{MnMoO}_6$, Sr_2MnWO_6 and Ca_2MnWO_6 : a neutron diffraction study. *J. Phys. Condens. Mat.* **2002**, *14*, 38, 8817-8830.
15. Lavat, A. E., Baran, E. J. IR-spectroscopic characterization of $\text{A}_2\text{BB}'\text{O}_6$ perovskites. *Vib. Spectrosc. A*. **2003**, *32*, 167-174.
16. Martinez-Lope, M. J., Alonso, J. A., Casais, M. T., Garcia-Hernandez, M., Pomjakushin, V. Preparation, structural study from neutron diffraction data and magnetism of the disordered perovskite $\text{Ca}(\text{Cr}_{0.5}\text{Mo}_{0.5})\text{O}_3$. *J. Solid State Chem.* **2006**, *179* ,8, 2506-2510.